Journal of Vertebrate Paleontology 19(4):654–665, December 1999


# ONTOGENETIC HISTOLOGY OF *APATOSAURUS* (DINOSAURIA: SAUROPODA): NEW INSIGHTS ON GROWTH RATES AND LONGEVITY

KRISTINA A. CURRY*
Department of Anatomical Sciences, Health Sciences Center, State University of New York at Stony Brook, Stony Brook, New York 11794-8081

ABSTRACT—The bone microstructure of an ontogenetic series of *Apatosaurus* radii, ulnae, and scapulae suggests that *Apatosaurus* underwent three distinct osteogenic phases. Primary laminar to plexiform fibro-lamellar bone tissue, devoid of lines of arrested growth (LAG), occurs in individuals up to 91% adult size. LAGs and longitudinally vascularized lamellar tissue are deposited for the first time in the external cortices of sub-adult individuals. Slow growth and additional deposition of accretionary lamellar bone occurs in adulthood, and indicates attainment of maximum size in *Apatosaurus*. All scapulae examined show cyclicity in vascularity indicative of regular variation in speeds of osteogenesis. In contrast, *Apatosaurus* radii and ulnae show consistent bone depositional rates throughout ontogeny. Despite inter-element variability, all *Apatosaurus* bones sampled corroborate the hypothesis of sustained rapid growth rates for most of ontogeny, followed by gradual decline with attainment of maximum size. Estimation of ages of ~10 years for large sub-adults refutes the hypothesis that slow, indeterminate growth was required for *Apatosaurus* and other sauropods to achieve extremely large body sizes.

## INTRODUCTION

Life history strategies employed by the immense Mesozoic sauropods have been hotly debated since the first description of *Cetiosaurus medius* (Owen, 1859). The suite of features associated with sauropod gigantism (Coombs, 1975; McMahon and Bonner, 1983; McIntosh, 1990a) has provided a considerable research impetus over the past 150 years. However, the lack of reasonable modern analogues renders most sauropod paleobiological hypotheses speculative at best. Mechanisms of sauropod growth and longevity are particularly difficult to address (e.g., Case, 1978; Bakker, 1980; Calder, 1984). Did sauropods grow indeterminately? Did sauropods grow at constant rates? Did they experience regular cycles of relative growth rate variation? How long did it take for them to reach adult size? Despite increasing interest and rigorous new methodologies, all of these questions have remained cloaked in mystery.

Sauropod bone histology may hold the keys to unraveling some of these paleobiological questions. Bone deposition and remodeling throughout ontogeny provides a window to the entire record of bone growth during the course of an individual's life history. In extant taxa, distinct bone tissue types are associated with different growth rates and patterns, and vertebrate bone tissue organization is readily preserved in the fossil record. The relationship between bone tissue pattern and depositional mechanisms has been conserved throughout vertebrate evolution (Amprino, 1940). Thus, when analogous tissue depositional patterns occur in extinct and extant taxa, bone growth rates and overall growth strategies in extinct taxa may be inferred (e.g., Ricqlès, 1977; Ricqlès et al., 1997).

The bone histology of the Sauropodomorpha (Prosauropoda + Sauropoda) is addressed in numerous articles (Owen, 1859; Seitz, 1907; Gross, 1934; Enlow and Brown, 1956, 1957, 1958; Currey, 1962; Ricqlès, 1968a, 1983; Reid, 1990; Chinsamy, 1993; Curry, 1994, 1996; Rimblot-Baly et al., 1995). However, the destructive nature of histological analysis and difficulty in handling extremely robust sauropod elements restricted previous investigations of sauropod bone histology to single element analyses, which preclude determination of generalized growth patterns for sauropod taxa. Although the value of histo-ontogenetic series of variable skeletal elements was realized early in the century (Nopsca, 1933), such comprehensive techniques have only rarely been rigorously applied to studies of dinosaurian growth (Varricchio, 1993).

In this study, I present an ontogenetic, histologic analysis of the sauropod dinosaur *Apatosaurus*. The bone microstructure of three appendicular elements among four age classes provides primary data on histovariability and allows the reevaluation of *Apatosaurus* ontogenetic growth dynamics. For the first time, histological differences among *Apatosaurus* skeletal elements throughout ontogenetic development are revealed. Results herein emphasize the possibilities for derivation of generalized growth patterns from bone microstructure of extinct taxa, and elucidate important aspects of the life history strategies employed by some of the largest terrestrial vertebrates ever to have inhabited the earth.

## MATERIALS AND METHODS

Twelve forelimb and pectoral girdle elements from at least four *Apatosaurus* individuals were used in this histological analysis. Two scapulae, three radii, and four ulnae were obtained from Brigham Young University's Cactus Park locality (BYU 641) in the Late Jurassic Brushy Basin Member of the Morrison Formation of Colorado. The Cactus Park bone bed yields disarticulated *Apatosaurus* sp. skeletal elements at various juvenile ontogenetic stages, and is hypothesized to represent a single event mass death assemblage (K. Stadtman, pers. comm., 1995). The Cactus Park specimens afford a unique opportunity to document osteogenic variation through progressive stages of juvenile ontogeny in a single *Apatosaurus* population, thus minimizing the possibility of histological differences due to ecological, environmental, or temporal variation.

A single adult specimen of *Apatosaurus excelsus* was included in the analysis in order to extend ontogenetic coverage. This specimen (University of Wyoming [UW] 15556) is approximately 25 m long and approaches the known maximum size for *Apatosaurus* (e.g., Colbert, 1962). The forelimb of this adult was found in articulation (Hatcher, 1902; Peterson and Gilmore, 1902; McIntosh, 1990b). The UW 15556 radius, ulna,

* Present address: Bell Museum of Natural History, 100 Ecology Building, University of Minnesota, St. Paul, Minnesota 55108.

TABLE 1. *Apatosaurus* age classes, derived from maximum bone length, muscle scar development and bone surface finish.

| Size class | Element | Maximum length (cm) | % adult size |
|---|---|---|---|
| I | radius R1 | 45.5 | 61 |
| | ulna U1 | 47.9 | 61 |
| | scapula S1 | 70.7 | 34 |
| II | radius R2 | 54.5 | 73 |
| | ulna U2 | 51.0 | 65 |
| | ulna U3 | 52.2 | 67 |
| | scapula S2 | 117.4 | 56 |
| III | radius R3 | 67.5 | 91 |
| | ulna U4 | 59.4 | 76 |
| IV | radius R4 | 74.2 | 100 |
| | ulna U5 | 78.5 | 100 |
| | scapula S3 | 210.9 | 100 |

and scapula provide data on bone histological variation among and within elements of a single *Apatosaurus* individual.

Inclusion of UW 15556 in the analysis introduces several assumptions. The lack of diagnostic characters in the Cactus Park specimens prohibits the assessment of species status, and no Cactus Park limb element can be confidently assigned to *Apatosaurus excelsus*. A posteriori recognition of identical histological trends in the Cactus Park specimens and *A. excelsus* allows the reasonable inclusion of UW 15556, despite ambiguous identification of the Cactus Park taxon. Such similar growth patterns are consistent with the assumption that all *Apatosaurus* followed comparable growth trajectories. It is not problematic to include two possibly different species.

Examination of radii, ulnae, and scapulae helps to overcome some methodological constraints associated with single-sample analyses. Not only are a wide range of biomechanical environments represented by individual elements, but different bones often undergo distinct patterns of deposition and resorption, which may result in disparate histological signals. Congruence of bone microstructure among different skeletal elements adds strength to hypotheses of generalized skeletal growth patterns.

Maximum bone length, as well as bone surface finish and muscle scar development, serve as measures of relative age status (Nopsca, 1933). Using these criteria, four age classes were identified. Age Class I (Early Juvenile) contains the smallest ulna, radius, and scapula from the Cactus Park locality. Age Class II (Late Juvenile) contains two Cactus Park intermediate-sized ulnae, one radius, and one scapula. Age Class III (Sub-Adult) consists of a radius and an ulna, both from Cactus Park and at least 75% adult size. No Class III scapula was available for sectioning. Age Class IV (Adult) consists of one ulna, one radius, and one scapula from UW 15556. See Table 1 for measurements of all elements.

The robust size of *Apatosaurus* limb material required slight modification of traditional paleohistologic technique (Ricqlès and Bolt, 1983). Unembedded bone samples were sectioned only as far as the central medulla of the mid-diaphyses on a 41-AR Buehler high speed diamond-blade saw. The resulting 6–8 cm bone block was removed with a hacksaw and small chisel. This technique allowed removal of bone only in the area of interest without destruction of maximum bone length or significant gross morphology. Transverse sections were made at standardized locations for each element: for the scapulae at the most proximal portion of the blade, and for radii and ulnae at 50% maximum bone length, in the central diaphysis (Fig. 1). Bone samples were then embedded in epoxy resin and several sections were made (3–4 mm thick) on the high speed saw. Sections were mounted and hand-ground on a lap wheel until the requisite optical contrast was obtained. Observations were made under a compound, petrographic microscope in ordinary and cross-polarized light.

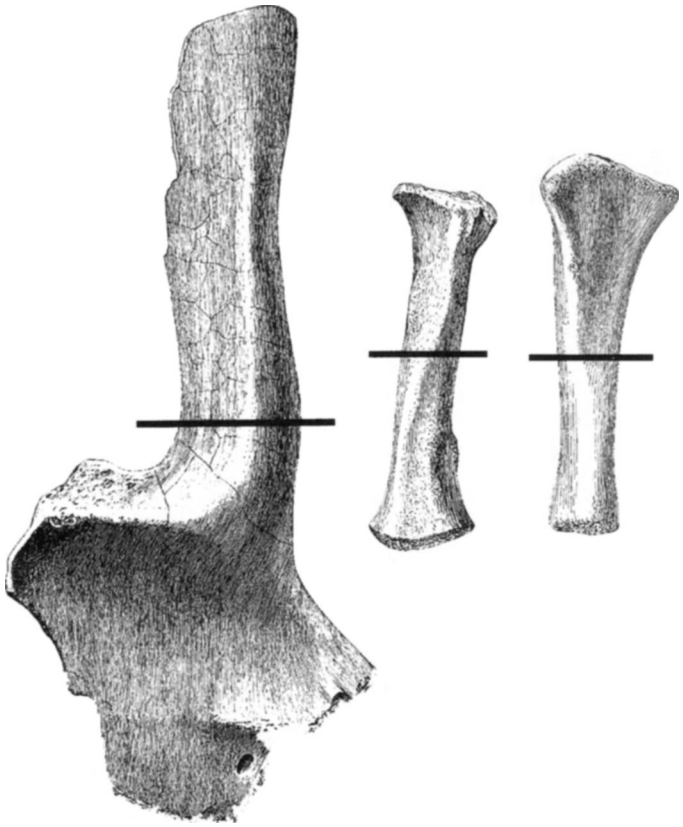

FIGURE 1. Area of thin-sections in scapula (right lateral view), radius (posterior view), and ulna (anterior view). Illustrations adapted from Gilmore (1936).

## RESULTS

For clarity, elements from a single age class are presented together. See Appendix One for a glossary of histological terms used in this text.

### Age Class I: Early Juveniles

**Radius and Ulna (R1, U1; Fig. 2)** —An extensive spongiosa exists in the deep medullary regions. Bony trabeculae lining marrow cavities are formed by a core of relatively older tissue at the axis of each trabecula, with newer, thin coats of endosteal bone at the periphery. The endosteal coating is always separated from the trabecular axis by a resorption line, indicating the involvement of erosion/reconstruction cycles in trabecular formation. The most superficial cavities of the spongiosa show osteoclastic invasion of the deep cortex via circular erosion rooms that directly communicate with the vascular canals of the primary cortex (Fig. 2A). The external cortex is entirely formed by primary tissue. Most vascular canals are surrounded by primary osteonal bone, and form a fibro-lamellar complex: primary osteons are embedded in a woven bone matrix (Fig. 2B). A two-dimensional network of longitudinal and circular vascular canals with occasional radial anastomoses permeates even the deep cortex to result in laminar to plexiform patterns of vascularity (Fig. 2B). Primary laminar/sub-plexiform tissue is visible beneath perimedullar secondary osteons. No lines of arrested growth (LAGs) occur in any region of the cross-section

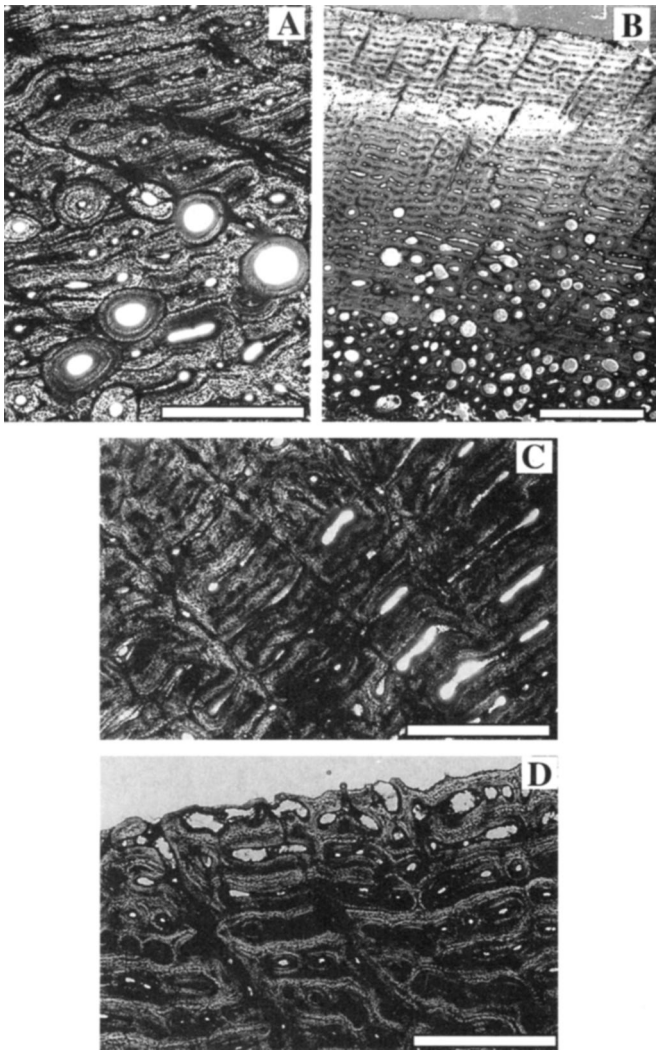


FIGURE 2. Age Class I radius and ulna. **A**, ulna showing perimedullar erosion. Laminar tissue underlies developing secondary osteons. No LAGS are observed. **B**, general view of cortical bone in cross section of Class I radius diaphysis. **C**, radius diaphysis, mid-cortex, showing laminar to plexiform vascularity in a fibro-lamellar context. **D**, subperiosteal view of radius with the external cortex exhibiting a woven bone matrix and open vascular network. Laminar to sub-plexiform vascularity predominates. No LAGS are present. Scale bars equal 100 μm.

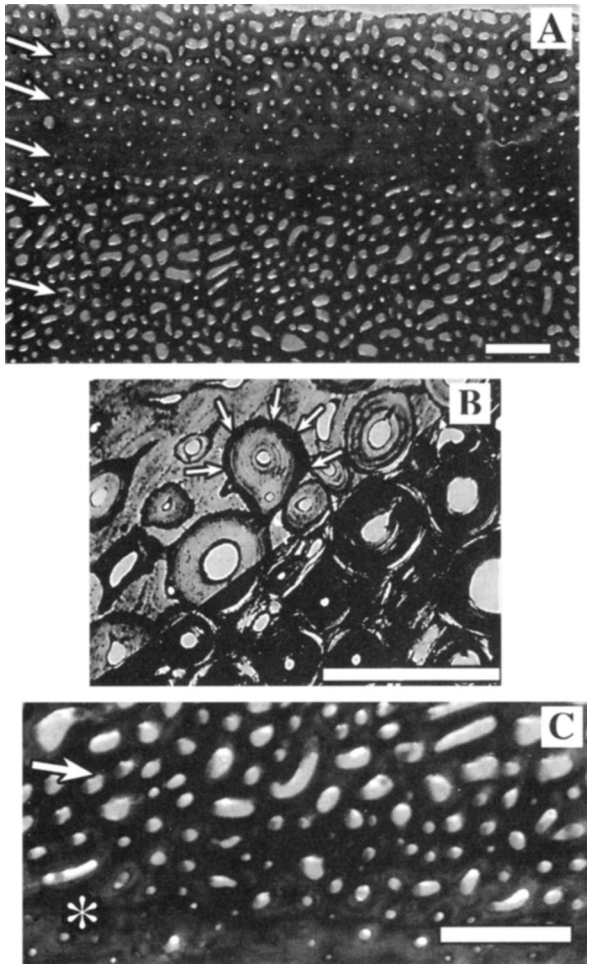


FIGURE 3. Age Class I scapula. **A**, general view of primary cortex. Well-vascularized fibrolamellar bone tissue exhibits cyclical variation in vascularity. Five cycles are marked by arrows; **B**, upper field of view: Haversian bone without crossed Nichols or polarized light. Lower field of view: Haversian osteons as seen with crossed Nichols and polarized light. A cementing line (arrows) marks the boundary of the secondary structure. Lamellar bone is indicated by fine dark and light banding (the axial cross surrounding a vascular canal); **C**, single vascular cycle. Area of longitudinal vascularity (marked by star) is followed by a wide region of laminar/reticular tissue (marked by arrow). Primary osteons in a woven matrix constitute the fibro-lamellar complex. Scale bars equal 100 μm.

(Fig. 2B, C). The primary bone is highly vascular, and consists of multiple rows of primary osteons embedded in a fibrous bone matrix of primary origin. The most peripheral bone tissue consists of a coarsely woven matrix and open vascular network, still exhibiting little osteonal deposition (Fig. 2D).

**Scapula (S1; Fig. 3)** —The scapula exhibits a gross histomorphology distinct from that of the radius and ulna. A central cancellous zone is sandwiched between two layers of compact cortex to result in a diploe. Four to five depositional cycles are notable at low magnification (Fig. 3A). The interior of the scapula is mostly cancellous bone, formed by highly organized trabeculae. Small cancelli are abundant in the deep scapula, and leave large marrow spaces between them. The trabeculae are secondarily endosteal. Each trabecular axis of primary tissue is surrounded by thin coats of more recently deposited endosteal bone. The endosteal nature of the peripheral trabecular bone is indicated by the presence of a resorption line. Differential resorption demonstrates an extensive anteroposterior drift of the marrow cavity as overall growth occurred. Most endosteally, some development of dense Haversian tissue obliterated primary bone (Fig. 3B).

Cycles in the scapula exhibit no annuli or LAGS, and are consistently fibro-lamellar. Local variation in osteogenic rate is recorded only by changing vascular patterns. Each growth cycle is formed by a narrow area of low vascularity, where canals are primarily longitudinal, with occasional reticular anastomoses. Wider regions of densely vascularized reticular and laminar tissue follow (Fig. 3A, C). Cycle thicknesses vary locally, and range from as thin as ~100 μm to maximum thicknesses of up to 4–5 mm. No complete cessation of appositional growth occurred. The number and diameter of vascular canals in primary cortical bone locally obscures the woven component of the fibro-lamellar complex, although it is readily viewable in cross polarized light.

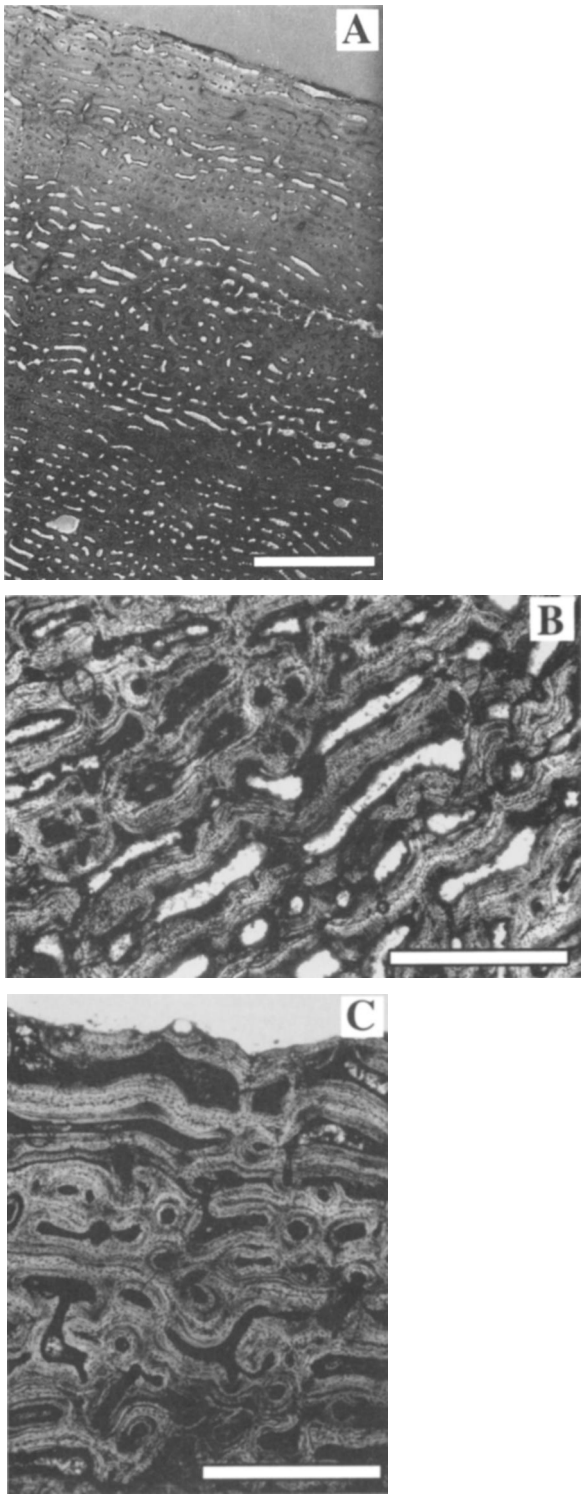


FIGURE 4. Age Class II radius and ulna. **A**, general view of cortex in an ulnar cross section. No LAGS or annuli are observed. Perimedullar vascular canals are widened by osteoclastic resorption, and some secondary osteons have replaced primary bone tissue most endosteally. **B**, detail of primary cortex in ulnae and radius. Bone exhibits a well-developed fibro-lamellar complex with laminar vascularization. **C**, ulna external cortex. An open-canal network exists sub-periosteally, with primary vascular canals not yet surrounded by osteonal material. Scale bars equal 100 μm.

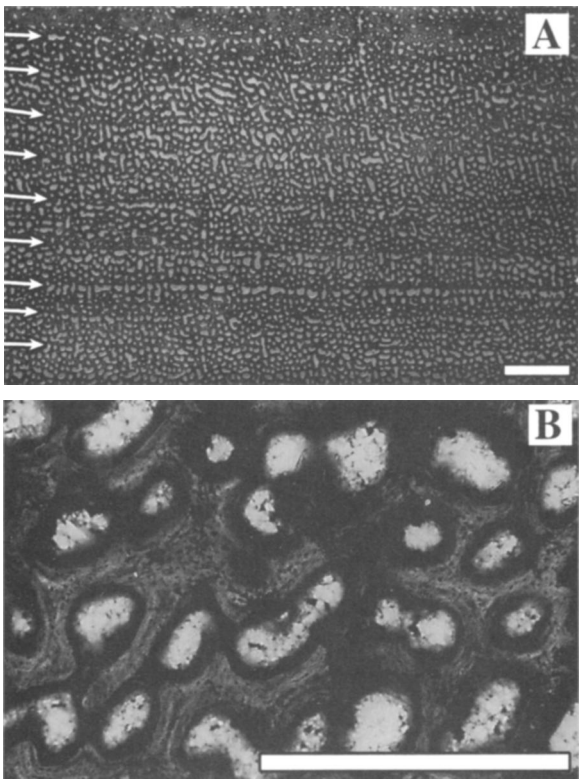


FIGURE 5. Age Class II scapula. **A**, general view of primary cortex. Ten growth cycles are indicated by arrows; **B**, detail of external primary cortex. Fibrolamellar bone is devoid of LAGS. Vascularity is dominated by longitudinal canals, but is locally laminar. Scale bars equal 100 μm.

### Age Class II: Late Juveniles

**Radius and Ulnae (R2, U2, 3; Fig. 4)** —In Age Class II, both radius and ulna show continued, uninterrupted appositional growth (Fig. 4A). The diaphyses of the ulnae and radius have undergone further endosteal reconstruction. Bony trabeculae are coated by endosteal bone, and large perimedullar erosion rooms are present. Formation of secondary osteons has resulted in locally dense Haversian tissue. Several generations of osteons overlie one another most endosteally. Bone resorption and redeposition of interstitial lamellae between third and fourth generation secondary osteons destroyed primary tissue in the innermost cortex. Laminar primary vascularity predominates between secondary osteons and in the outer cortex (Fig. 4A, C). Different vascular regions interweave and are not demarcated by annuli and/or LAGs. Periosteal bone is characterized by dense accumulations of osteocyte lacunae with extensive canalicular networks. Most periosteally, an open network of vascular canals persists. Vascular lumens surrounded by circumferentially organized lamellae and osteocyte lacunae and devoid of cementing lines are differentiated as primary osteons. Embedded in woven matrices, they form the typical fibro-lamellar bone tissue complex (Fig. 4B, C).

**Scapula (S2; Fig. 5)** —The scapula is composed of tissue identical to that seen in the Class I scapula (Fig. 5A, B). There are 8 to 10 cycles in S2, as compared to only four or five in S1 (Figs. 3A, 5A). Cycle counts for both scapulae were made in the regions of the most complete cortical record. Cycles exposed in the deep cortices of S1 and S2 may indicate the same depositional events (Fig. 6A, B). In addition, the marrow cavity continues an anterolateral drift, as indicated by the anterolateral erosion of periosteal tissue and posteromedial deposition of

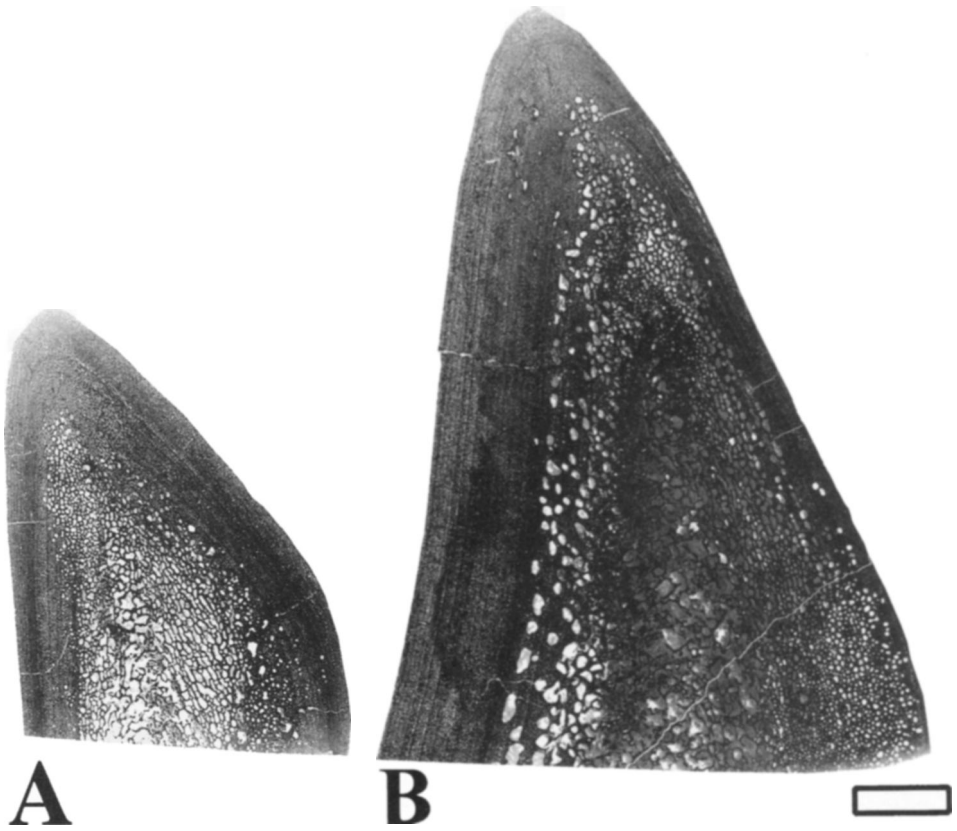


FIGURE 6. **A**, gross view of Age Class I Scapula cross-section. Four to five cycles are viewable on the medial surface of the element. **B**, gross view of Age Class II Scapula cross-section. Ten cycles are viewable on the medial surface of the element. Scapula 2 experienced extensive anterolateral remodelling. In both elements, cycle thicknesses vary from ~100 μm to 4–5 mm. Scale bar equals 1 cm.

endosteal bone. The diploic structure is again well-developed with medial and lateral cortical walls surrounding a large spongiosa.

### Age Class III: Sub-Adults

**Radius and Ulna (R3, U4; Fig. 7)** —The radius and ulna of Class III *Apatosaurus* show the first evidence of slowed bone deposition. A dense spongiosa comprises the marrow cavity of both the radius and ulna. Bony trabeculae have undergone multiple erosional and redepositional events, as indicated by multiple layers of superimposed secondary tissue. In the deepest cortex, no primary tissue persists (Fig. 7A). The inner cortex merges progressively with the spongiosa at the endosteal margin. The cortex is thick and comprised of two regions with distinct vascular patterns. The deep cortex is formed by dense Haversian bone tissue (Fig. 7A). Reconstruction of primary canals has resulted in mostly longitudinally-oriented secondary osteons. Each vascular canal is surrounded by secondary lamellar osteonal material, as indicated by the resorption lines at the external periphery of each secondary osteon (=Haversian system). Substitution of primary osteons occurs even in localized regions of the outer cortex (Fig. 7B). The outer cortex lies superficial to dense Haversian tissue of the inner cortex and contains the first evidence of annuli and LAGs (Fig. 7B, C). The deepest periosteal cortex is fibro-lamellar and contains dense vascularization by primary osteons with predominately circular and longitudinal orientations. The outermost cortex is parallel or locally lamellar fibered. Several annuli are visible, followed by at least two to three LAGs (Fig. 7C). Vascularization becomes more sparse in areas of annuli and LAGs, and is primarily longitudinal. Following the annuli and LAGs present in the outer cortex, localized fibrolamellar deposition resumes at the sub-periosteal surface, although vascularity remains longitudinal (Fig. 7C). Secondary osteons invade the external cortex in localized regions (i.e., the posterior anconeal spine of the ulna).

### Age Class IV: Adult

**Radius and Ulna (R4, U5; Fig. 8)** —The diaphyses of both radius and ulna from this adult individual are comprised of several distinct regions. The spongiosa is formed of numerous thick trabeculae, with a complex structure recording numerous episodes of erosion and endosteal redeposition (Fig. 8A). The cortex is mostly dense Haversian tissue. Interstitial lamellae from pre-existing Haversian osteons have replaced primary tissues in deep cortical regions. However, in isolated regions, fibro-lamellar tissue persists between the secondary osteons (Fig. 8B). Primary tissue between developing secondary osteons in the periosteal cortex is lamellar and punctuated with multiple LAGs (Fig. 8C). An exact count of LAGs is impossible, due to obliteration during reconstruction. Vascularity at the outermost cortex is sparse and longitudinal (Fig. 8B).

**Scapula (S3; Fig. 9)** —The microstructure of the adult scapula is observable in restricted regions that represent deep, middle, and superficial cortices. The spongiosa is formed by thick trabeculae indicating multiple cycles of erosion and redeposition. Endosteally coated marrow spaces lie between bony trabeculae and form sinuses of various diameters (Fig. 9A). Primary tissue, when observable beneath Haversian osteons in the mid-cortex, is fibro-lamellar. The most periosteal regions are

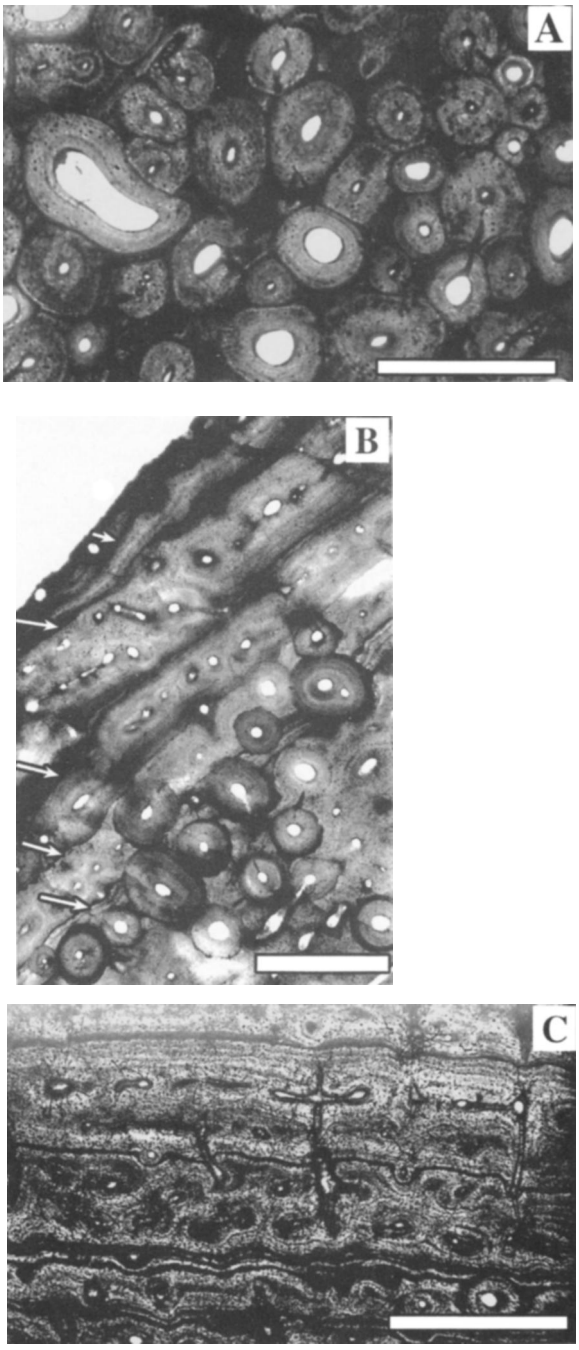


FIGURE 7. Age Class III radius and ulna. **A**, ulnar deep cortex. Dense Haversian tissue and interstitial lamellae obliterate most of primary bone tissue. **B**, detail of radius diaphyseal cortex. Annuli and LAGs (marked by arrows) are common in sub-periosteal bone tissue. Lamellar matrix most externally, with longitudinal vascularization. **C**, detail of LAGs at the periostic border of ulna. Annuli and LAGs are followed by periosteal deposition of parallel–woven fibred bone tissue. Osteocyte lacunae in regions of LAGs are flattened, with few canalicular anastomoses. Scale bars equal 100 μm.

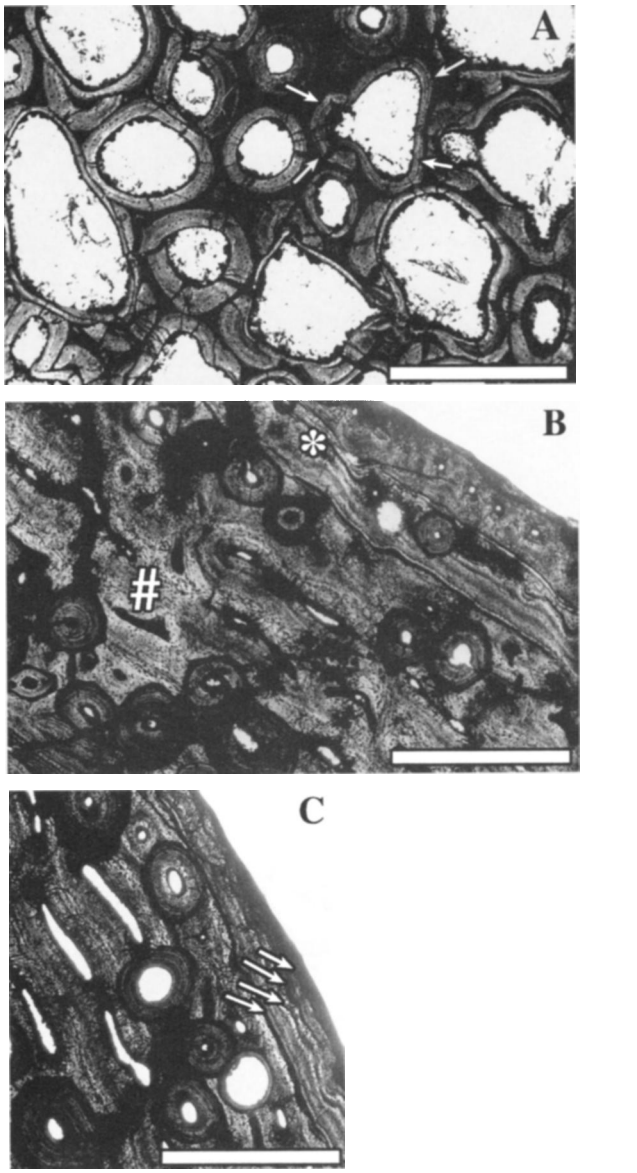


FIGURE 8. Age Class IV ulna and radius. **A**, spongiosa composed of numerous trabeculae. Trabecular axes have been reconstructed. Arrows indicate resorption lines and periphery of endosteal bone tissue. **B**, detail of mid-cortical bone tissue in an adult ulna. Haversian osteons extend into external cortex. Primary tissue underlies osteons and is fibro-lamellar endosteally (#), and lamellar externally (*). Several LAGs punctuate the external cortex and are preceded and followed by lamellar-fibred bone tissue with longitudinal vascularity. **C**, detail of external cortex in an adult radius. Multiple accretionary LAGs are present in a lamellar bone matrix (arrows). Scale bars equal 100 μm.

well-preserved and differ markedly from Age Class I and II scapular histomorphology. Canals are sparsely developed and exclusively longitudinal (Fig. 9B). The fibro-lamellar complex exhibited by juvenile scapulae and the middle cortex of this sample is not present. Instead, S3 periosteal bone exhibits distinct zones demarcated by multiple LAGs. Tissue is increasingly avascular and deposited in thin parallel lamellae (Fig. 9C). Useful LAG counts could not be obtained.

## DISCUSSION

Several features of *Apatosaurus* bone microstructure elucidate aspects of sauropod growth rates, longevity, and histovariability. Three main phases of osteogenesis occurred during *Apatosaurus* ontogeny (Table 2). Relative age classes inferred a priori from overall bone size and morphology are upheld by corresponding bone microstructural variation. Despite histological variability among skeletal elements, all observations cor-

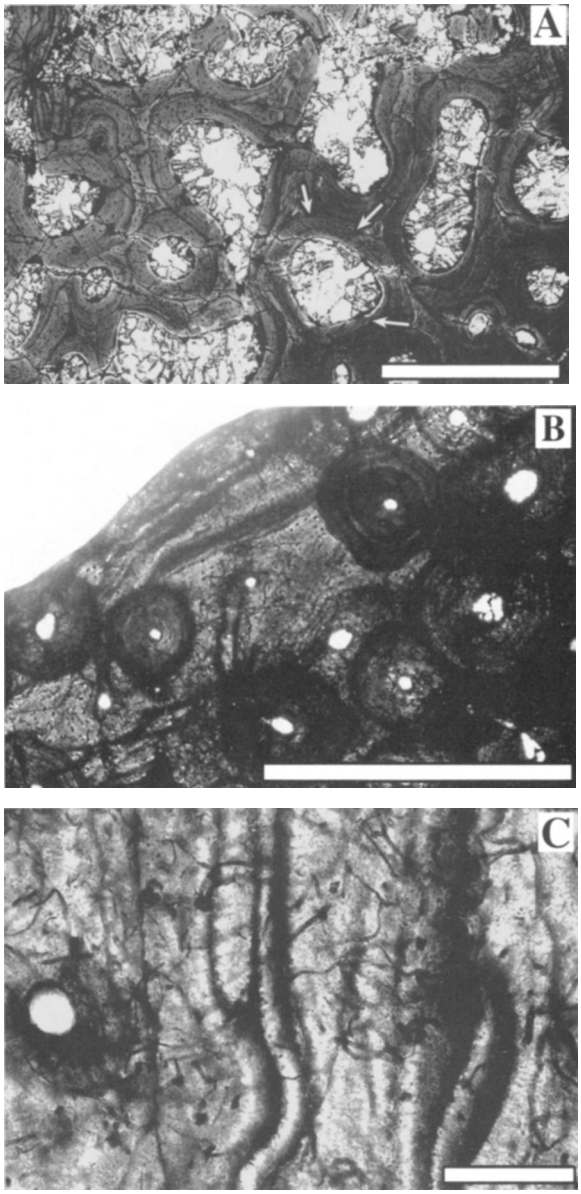


FIGURE 9. Age Class IV scapula. **A**, spongiosa in adult scapula. Marrow cavities are surrounded by layers of endosteal bone (arrows); **B**, external cortex. Haversian osteons and LAGs extend to the periosteal margin of the cross-section; **C**, lamellar tissue of external cortex. Osteocyte lacunae are flattened. Longitudinal canals are sparse and often surrounded by secondary osteons. Scale bars (A and B) equal 100 μm. Scale bar (C) equals 10 μm.

roborate sustained, rapid bone growth until late *Apatosaurus* ontogeny followed by a declining growth rate and probable plateau in adulthood. *Apatosaurus* gross bone depositional patterns allow a non-traditional reconstruction of sauropod biology.

### *Apatosaurus* Ontogenetic Growth Strategy

Three distinct growth regimes characterize *Apatosaurus* ontogeny. In Growth Stage A, rapid deposition of primary fibro-lamellar bone tissue with predominately laminar to locally subplexiform vascularity occurs in individuals up to 73% adult size (Age Classes I and II). No LAGs or annuli are present in the elements examined. This sustained, rapid growth pattern comprises the bulk of bone growth in *Apatosaurus*. Growth Stage B is evident in Class III individuals (up to 91% adult size). Haversian reconstruction occurs throughout the cortex and is most pronounced endosteally. Parallel-fibred bone, annuli, and sparse longitudinal vascularization dominate the most external periostic cortex. Following initial LAGs, fibrolamellar regions with sub-laminar vascularity persist in localized regions. In Growth Stage C (Class IV) new bone tissue is primarily avascular and/or longitudinally vascularized lamellar bone. Multiple generations of Haversian reconstruction extend into the periostic cortex. LAGs at the sub-periosteal surface indicate local cessation of appositional growth. Lamellar annuli precede and follow LAGs. This suite of features occurs exclusively in radii, ulnae, and scapulae of Age Class IV *Apatosaurus*.

TABLE 2. *Apatosaurus* bone microstructural growth stages.

| |
|---|
| Growth Stage A: Age Classes I and II (individuals up to 73% adult size) |
| primary deposition of fibro-lamellar bone |
| laminar to plexiform vascularity |
| no annuli or LAGs |
| Haversian bone only at endosteal margin |
| Growth Stage B: Age Class III |
| Haversian reconstruction throughout cortex |
| primary fibro-lamellar bone for ~75% of cortical deposition |
| parallel-fibered bone at periosteal surfaces |
| annuli and LAGs at periosteal surface |
| decrease in vascularity to primarily longitudinal post-LAGs |
| Growth Stage C: Age Class IV |
| dense Haversian tissue extensively developed |
| primary deposition of lamellar bone at periosteal surface |
| periosteal bone is avascular |
| accretionary bone deposits at periosteal margin |
| periosteal bone marked with multiple annuli and LAGs |

The *Apatosaurus* osteogenic pattern of uninterrupted, highly vascularized fibro-lamellar tissue deposition, gradually declining to poorly vascularized, lamellar tissue by adult stages indicates a commensurate variation in general body growth patterns during ontogeny. Body growth rate is related to primary bone growth rate which, in turn, is expressed by histologic structures and vascular patterns (Amprino, 1947). Higher rates of periosteal osteogenesis are indicated by less spatially organized organic matrices with abundant vascular canals in several directions. Conversely, highly organized fibrillar matrices and poor vascularization indicate slower rates of periosteal bone formation. Fortunately, both aspects of bone microstructure are preserved in *Apatosaurus,* and aid in determination of qualitative bone growth rates.

Fibro-lamellar bone predominates throughout *Apatosaurus* ontogeny. The original cancellous composition of fibro-lamellar tissue allows a greater volume of new periosteal bone deposition than would a more compact tissue (Ricqlès, 1975, 1977; Francillon-Vieillot et al., 1990). Fibro-lamellar tissue is most commonly observed in extant taxa with rapid overall body growth. In most large mammals and birds, typical fibro-lamellar bone is formed continuously throughout active phases of postnatal growth (Peabody, 1961; Castanet et al., 1993; Castanet et al., 1995; Sanchez-Herraiz et al., 1997). Fibro-lamellar bone has been observed in crocodylians (Reid, 1997), but is normally zonal in nature, with cyclically-developed fibro-lamellar growth zones bounded by annuli and/or LAGs (Buffrénil, 1980; Ferguson et al., 1982). The presence of fibro-lamellar tissue in *Apatosaurus* follows the bone tissue–growth rate relationship (Amprino, 1947), and indicates an overall rapid increase in bone and body size until late sub-adult ontogeny.

Sustained, rapid skeletal growth during *Apatosaurus* ontogeny is also diagnosed by the vascular patterns present in radii, ulnae, and scapulae. *Apatosaurus* vascular patterns in Growth

Stages A and B indicate rapid deposition. The complexity of vascular canal arrangements in extant taxa and dinosaurs is used as a qualitative estimate of relative speeds of fibro-lamellar deposition (e.g., Currey, 1960; Ricqlès, 1977; Reid, 1981, 1996; Chinsamy, 1990, 1993, 1995; Varricchio, 1993; Horner et al., 1997; Ricqlès et al., 1997). Ricqlès (1975) divides fibro-lamellar bone (sensu Gross, 1934) into plexiform and laminar varieties, based on the orientations of vascular canals. In plexiform tissue, radial anastomoses are conspicuous and create a canal network that supplies the growing tissue with abundant vascularization in three-dimensions. Laminar tissue lacks a radial canal component and forms a two-dimensional vascular network. Laminar fibro-lamellar bone is the fastest growing osseous tissue (Castanet et al., 1996). Uninterrupted deposits of laminar-plexiform fibro-lamellar bone in Age Classes I and II are thus hypothesized to indicate an elevated growth rate in *Apatosaurus,* approximating that of large modern mammals and birds, and exceeding that of most feral crocodylians, chelonians, and lepidosaurs (e.g., Currey, 1962; Ricqlès, 1968a, 1980; Rimblot-Baly et al., 1995).

Secondary (Haversian) tissues in all *Apatosaurus* Age Classes indicate local variation in bone growth patterns, as well as more general trends in bone deposition, resorption, and remodelling during ontogeny. Distributions of Haversian osteons range from scattered to dense, in Age Classes I–IV, respectively. Even the most superficial cortices in Age Class IV radius and ulna contain dense Haversian tissue. Haversian substitution is most common in extant mammals and is only weakly developed in other tetrapods (Enlow and Brown, 1956, 1957, 1958; Ricqlès, 1991). Haversian reconstruction is a time-dependent process: as more time elapses, the probability that primary bone tissue will be reconstructed increases. It is most frequently linked to age, muscle attachment, and mineral storage and processing (Amprino, 1948; Lacroix, 1971; Martin and Burr, 1989). In addition, Haversian bone is hypothesized to offer numerous biomechanical advantages as mass increases. Extensive bone remodeling may be crucial to maintenance of bone integrity under massive loading (Evans and Riolo, 1970). Such characteristics of Haversian bone may be particularly advantageous to large-bodied *Apatosaurus* with masses in excess of 28,000 kg (Colbert, 1962). Haversian substitution in *Apatosaurus* is probably the result of a combination of these processes (Ricqlès, 1980).

*Apatosaurus* Age Class III and IV (>75% adult size) ulnae, radii, and scapulae show the first evidence of declining bone growth rates. Sub-adult deposits of annuli, LAGs, and parallel and/or lamellar fibered matrices are followed by deposition of lamellar accretionary bone into adulthood. The transition from laminar and sub-plexiform tissues (Age Classes I and II) to poorly vascularized lamellar tissue with annuli and LAGs suggests an overall decrease in *Apatosaurus* periosteal osteogenesis. In extant taxa that stop growing after reaching a maximum size, minor thickening of bone may still occur by accretion of small amounts of poorly vascularized lamellar bone tissue (the "external fundamental system" in treatises of human histology). Accretionary, circumferential lamellar bone is hypothesized to be the strongest bone in the skeleton (Carter and Spengler, 1978). A low porosity and lamellated structure predispose accretionary bone to resist loads in vivo, and may serve a significant role in maintenance of structural integrity in *Apatosaurus* bone. In addition, avascular, peripheral accretionary bone is often marked with LAGs and resorption lines and is associated with growth rate plateaus in extant taxa (Enlow and Brown, 1956, 1957, 1958). As in modern mammals and birds, *Apatosaurus* accretionary tissue may indicate a growth plateau, and attainment of maximum size.

An additional type of cortical stratification was observed in all size classes of *Apatosaurus* scapulae. Scapular growth mirrors continuous fibro-lamellar deposition in Age Classes I, II, and III radii and ulnae. In *Apatosaurus* scapulae, however, a regular variation of continual deposition is indicated by variable vascular patterns arranged as superimposed cycles of growth. Regions of relatively slower growth exhibit longitudinal vascularity while areas of faster growth exhibit more extensive canal networks. Cycles are not marked by LAGs or clear annuli.

Similar cortical stratification has been noted in sirenians (Fawcett, 1942), leatherback turtles (Rhodin, 1985), ichthyosaurs (Buffrénil and Mazin, 1990), and in other sauropods (Ricqlès, 1968a, 1983; Reid, 1981; Rimblot-Baly et al., 1995). Rhodin (1985) concluded that such structures reflect cyclical growth of primary cortices, with faster and slower growth periods. Such cycles in sauropod taxa record mild modulations of bone deposition in a framework of fast (to very fast) growth. *Apatosaurus* scapular zonation must be considered in the context of rapid continuous bone deposition: primary periosteal bone is consistently fibro-lamellar, and devoid of LAGs and annuli. Cycles in *Apatosaurus* scapulae are not equivalent to cycles resulting from a steep drop in bone formation, as commonly observed in extant poikilotherms (Peabody, 1961; Castanet and Naulleau, 1985; Castanet and Smirina, 1990) and some dinosaurs (*Syntarsus*: Chinsamy, 1990; *Troodon*: Varricchio, 1993; or *Massospondylus*: Chinsamy, 1993).

### *Apatosaurus* Histovariability

In addition to information on overall *Apatosaurus* growth strategy, this study highlights histologic variability among three sauropod skeletal elements. Such variation in bone histology among elements of the same individual and similar-sized animals of the same taxon should be expected and explained by rigorous histologic analyses. Bone tissue typologies are the result of complex genetic and epigenetic interactions (cf. Ricqlès et al., 1991), and depositional patterns are controlled by phylogenetic, functional, and biomechanical constraints. Therefore, all of the above must be considered in the analysis of final osteogenic patterns (Horner et al., 1997; Ricqlès et al., 1997a, b).

The inclusion of the articulated adult *Apatosaurus* (UW 15556) corroborates histovariation observed within each age class. While radii and ulnae within each class grew continuously at sustained rates, scapulae exhibit cyclical growth rate variation. Each scapular cycle corresponds to the fast-growth, laminar and plexiform tissue observed in elements of the forelimb, but presents histomorphology distinct from that of radii and ulnae: Scapular areas of slightly less abundant vascularization are viewable at low magnification, instead of the uniform composition notable in radii and ulnae.

Scapulae, radii and ulnae in the sample all form via initial endochondral ossification, although with significantly different morphological results. The scapulae form as flat bones, with a central diploe structure surrounded by inner and outer cortical tables. Long bones, however, are not diploic. Extensive development of medullary spongiosa occurs in the *Apatosaurus* radii and ulnae. Scapular cyclicity may be attributed, in part, to variable shape and topological requirements in growth dynamics among the different elements (Reid, 1981; Ricqlès, 1983).

Some differences in primary tissues among scapulae, radii, and ulnae may be attributed to their biomechanical environments throughout ontogeny. Primary, woven bone tissue is more fatigue resistant than Haversian and other secondary tissues (Carter et al., 1976). The ulna was the primary weight-bearing bone of the sauropod forelimb, and retained a relatively greater woven primary tissue component in late ontogeny, while similar-sized radii experienced vast reconstruction with secondary tissues. Similarly, elaboration of Haversian tissues and accretionary lamellar bone may provide different mechan-

ical advantages for accommodating large compressive loads accompanying heavy masses in sauropods.

This histological analysis of *Apatosaurus* underscores the need for rigorous sampling of skeletal elements of extinct and extant taxa to gain a more complete understanding of fossil bone tissue types. In contrast to abundant LAGs noted in sauropod pelvic elements (Reid, 1981), typical LAGs are not notable in *Apatosaurus* radii, ulnae, and scapulae, until accretionary bone deposits occur in late ontogeny. Sections of other *Apatosaurus* elements may indeed reveal true LAGs. Asynchronous bone deposition often occurs in different skeletal elements, and may result in an erroneous assignment of ages when single bones are sampled. Obviously sections from single elements are unreliable in delimiting statements on overall growth. Recent works (e.g., Castanet et al., 1996; Crompton et al., 1996) on avian histogenesis reveals that while some bones in a single skeleton may deposit LAGs, others may not undergo substantial microstructural modification. In fact, even LAG counts within elements of a single individual may result in different biological age estimates! Because we can only observe growth dynamics within isolated thin-sections, the more elements and section-per-element, the more comprehensive the histologic resolution. Systematic, inclusive analyses are imperative to outlining overall growth dynamics in extinct taxa.

### *Apatosaurus* Longevity

Increasing degree of secondary substitution (remodeling), overall bone histomorphology, and cycle and/or LAG counts have been frequently used as indicators of relative and absolute ages in dinosaurs (e.g., Chinsamy, 1990; Varricchio, 1993; Curry, 1995). Differences in histologic organization of cortical periosteal primary tissues in *Apatosaurus* scapulae, radii, and ulnae have implications for relative and absolute age determination. Similarly, cycles documented in *Apatosaurus* scapulae allow the estimation of absolute ontogenetic age. Analogy to normal cyclicity in extant taxa allows the reasonable assumption that each cycle in *Apatosaurus* scapulae represents a single year or seasonal deposition. Cycle counts, or ages, are 5 and 10 in Class I and II scapulae, respectively. In contrast, radii and ulnae show no cyclicity. Had only radii and ulnae been examined under the assumption that a single cycle/LAG indicates yearly events, it could be concluded that up to 91% of *Apatosaurus* skeletal growth occurred prior to completion of the hatching year! Histological comparison with scapulae reveals an inter-element age discrepancy, and indicates that radii and ulnae may instead reflect multiple years of continuous bone deposition. Examination of multiple skeletal elements allows a more detailed age analysis.

As primary bone tissue is obliterated throughout ontogeny by remodelling and secondary tissue deposition, cycles deposited early in ontogeny are usually lost. Ontogenetic series allow potential gaps in the cortical record to be accounted for: earlier growth stages yield insights into bone tissue structure in remodelled regions of older elements. Endosteal reconstruction characterizes scapulae from Age Classes I and II (more extensively in S2). In deep regions of S1, primary bone tissue underlies newly-formed trabeculae and secondary osteons. Since no additional cycles are observed in this deep primary tissue, there is a high degree of confidence in cycle count accuracy. Therefore, a maximum count of five cycles serves as a minimum age estimate of five years for S1. Similarly, 8–10 countable cycles are preserved on the medial surface of S2. Despite considerable lateral reconstruction in S2, the relatively complete medial record allows correlation of cycle counts in S1 and S2. Because trabecular remodeling and medullary expansion occurs primarily on the lateral surface of S2, it is possible that the first five cycles present in Scapula 2 are equivalent to the five cycles noted in Scapula 1. Even if this is not the case, no more than five or six cycles of the same width could have been eroded in Scapula 2, and maximum cycle count would not exceed 16. Thus, the minimum age estimates derived from cycle counts are five and ten years for S1 and S2, respectively (Figs. 3A, 5A, 6A, B).

### Sauropodomorpha Histology: Comparative Analysis

Analyses of sauropod bone microstructure have identified a diversity of bone tissue types similar to that found in all extant vertebrates (see Ricqlès, 1980 for an historical summary). Reliance on single skeletal elements has precluded satisfactory resolution of overall sauropod growth strategy. Only two analyses have provided information on sauropodomorph ontogenetic histology (Chinsamy, 1993; Rimblot-Baly et al., 1995). Several important distinctions from these previous sauropod histological analyses are notable in the present study of *Apatosaurus* bone microstructure. Chinsamy's (1993) examination of *Massospondylus* femoral ontogeny yielded a pattern of cortical stratification consisting of zones, annuli, and LAGs indicative of complete cessation of local osteogenesis at intervals throughout life history. Although growth zones narrow externally in *Massospondylus* adults, no accretionary lamellae exist at the cortical periphery. Thus, Chinsamy hypothesized an indeterminate growth pattern. Histological incongruence occurs between *Massospondylus* femora and other prosauropod bones (ribs, vertebrae, unidentified limb material) that exhibit continuous deposition similar to that seen in *Apatosaurus* (Currey, 1962; Ricqlès, 1968). Variation among prosauropod skeletal elements precludes conclusive determination of *Massospondylus* growth strategy. However, the congruence of patterns among radii, ulnae, and scapulae of *Apatosaurus* supports the bone depositional strategy proposed here.

An analysis of bone microstructure in "*Lapparentosaurus madagascariensis*" humeri (Rimblot-Baly et al., 1995) is the only ontogenetic analysis of sauropod histology available for comparison. Interestingly, "*Lapparentosaurus*" humeri exhibit a cortical stratification similar to that observed in *Apatosaurus* scapulae. Rimblot-Baly et al. (1995) also noted lamellar, accretionary tissue at the cortical periphery in their largest samples identical to that observed in *Apatosaurus* bone. Despite their interpretation of these tissues as indicative of attainment of a maximum size, they hypothesized an indeterminate growth pattern in "*Lapparentosaurus.*" In epiphyseal sections made of a middle-sized humerus (60 cm long), they noted the presence of hypertrophied calcified cartilage. These epiphyseal sections probably are consistent with continued longitudinal growth. However, the element under consideration was only ~50% adult size (1.20 m), and attainment of adult stature requires continued bone elongation. I interpret the adult diaphyseal histology, of both *Apatosaurus* and "*Lapparentosaurus,*" as indicative of a determinate pattern of growth. Acceptance of an hypothesis of indeterminate longitudinal growth in either taxon must be supported by epiphyseal microstructure congruent with bone elongation in adult age classes. In both sauropods, rapid, continuous osteogenesis throughout ontogeny is followed by a gradual decline into adulthood. Exclusive deposition of primary accretionary lamellar bone occurs in both taxa in sub-adult and adult ontogenetic stages.

## CONCLUSIONS

This analysis of *Apatosaurus* bone histology clarifies ontogenetic osteogenesis in this Jurassic sauropod giant. The predominance of fibro-lamellar laminar and plexiform bone tissue devoid of LAGs and annuli indicates a sustained, rapid rate of osteogenesis until a late sub-adult ontogenetic stage. Deposition of lamellar-fibered accretionary bone occurs in the cortical pe-

ripheries of sub-adult and adult *Apatosaurus* scapulae, radii, and ulnae. When viewed in the context of rapid bone development for most of ontogeny, lamellar accretionary bone and LAG deposits may indicate a determinate growth pattern in the elements studied.

In addition to overall osteogenesis, this study provides additional information regarding histovariability among three *Apatosaurus* skeletal elements. Laminar, fibro-lamellar bone tissue in all elements indicates sustained rapid growth. Cyclicity of scapulae is reflected in slight variation in vascular patterns. Radii and ulnae exhibit no cyclicity. Cycle counts in scapulae give minimum longevity estimates of eight to ten years for *Apatosaurus* to reach sub-adult sizes.

Congruence of bone microstructural patterns among all elements examined corroborates an hypothesis of overall skeletal growth in *Apatosaurus,* and refutes the long-standing hypothesis of requisite *Apatosaurus* lifespan extension for the attainment of extremely large body size. Rapid bone growth throughout ontogeny was followed by a gradual growth plateau beginning at around age eight to ten. *Apatosaurus* attained a maximum size, and probably plateaued well within the temporal limitations associated with maximum size acquisition in extant mammals and birds.

## ACKNOWLEDGMENTS

My greatest gratitude goes to my undergraduate advisor at Montana State University, Dr. Jack Horner, who provided enthusiasm, guidance, trust, incredible scientific opportunities, and support throughout this endeavor. I thank Brent Breithaupt and Ken Stadtman for allowing access to *Apatosaurus* bones for histological sectioning. I greatly appreciated stimulating discussions and suggestions provided by Drs. Armand de Ricqlès and Jacques Castanet. Special thanks to Ellen Lamm, who taught me everything I know about histo lab techniques, was the supplier of innumerable bandaids for ground away fingertips, and was an irrepressible friend and supporter throughout this study. Thanks to B. Breithaupt, J. Castanet, J. Horner, M. O'Leary, A. de Ricqlès, S. Sampson, M. Schweitzer, and D. Varricchio for helpful comments on earlier versions of this manuscript. Editorial advice and suggestions from Cathy Forster, Dave Krause, and Ray Rogers greatly improved the quality of this paper and are very much appreciated, and the manuscript benefited from careful reviews by J. Castanet, A. Chinsamy, A. de Ricqlès, and R. Reid. Thanks also to Luci Betti for assistance with illustration preparation. This research was facilitated by NSF# EAR-9219035 to J. R. Horner, and was completed with financial support from the S. U. N. Y.-Stony Brook Gabor Inke Graduate Research Fellowship.

## LITERATURE CITED

Amprino, R. 1947. La structure du tissu osseux envisagée comme expression de différences dans la vitesse de l'accroissement. Archives de Biologie 58:315–330.

——— 1948. A contribution to the functional meaning of the substitution of primary by secondary bone tissue. Acta Anatomica 5 (III): 291–300.

Bakker, R. T. 1980. Dinosaur heresy—dinosaur renaissance: Why we need endothermic archosaurs for a comprehensive theory of bioenergetic evolution; pp. 351–462 *in* R. D. K. Thomas and E. C. Olson (eds.), A Cold Look at the Warm-Blooded Dinosaurs. AAAS Selected Symposium, Vol. 28. Westview Press, Boulder.

Buffrénil, V. de. 1980. Mise en évidence de l'incidence des conditions de millieu sur la croissance de *Crocodylus siamensis* (Schneider, 1801) et valeur des marques de croissance squelettiques comme indicateur de l'âge individuel. Archives de Zoologie Experimentale et Génerale 121:63–76.

——— and J-M. Mazin. 1990. Bone histology of the ichthyosaurs: comparative data and functional interpretation. Paleobiology 16(4): 435–447.

Calder, W. A., III. 1984. Size, Function, and Life History. Harvard University Press, Cambridge, 431 pp.

Carter, D. R., and D. M. Spengler. 1978. Mechanical properties and chemical composition of cortical bone. Clinical Orthopedics and Related Research 135:192–217.

———, Hayes, W. L., and D. J. Schurman. 1976. Fatigue life of compact bone-II. Effects of microstructure and density. Journal of Biomechanics 9:211.

Case, T. J. 1978. Speculations on the growth rate and reproduction of some dinosaurs. Paleobiology 4:320–328.

Castanet, J., and G. Naulleau. 1985. La squelettochronologie chez les Reptiles. II—Résultats expérimentaux sur la signification des marques de croissance squelettiques utilisées comme critère d'âge chez les serpents. Remarques sur la croissance et la longévité de la Vipère Aspic. Annales de Sciences Naturelle Zoologie (Paris) 7: 41–62.

——— and A. de Ricqlès. 1986–1987. Sur la relativité de la notion d'ostéones primaires et secondaires et de tissu osseux primaire et secondaire en général. Annales de Sciences Naturelles, Zoologie (Paris) 8:103–109.

——— and E. Smirina. 1990. Introduction to the skeletochronological method in amphibians and reptiles. Annales de Sciences Naturelles, Zoologie (Paris) 11:191–197.

———, H. Francillon-Viellot, F. J. Meunier, and A. de Ricqlès. 1993. Bone and individual aging; pp. 245–283 *in* B. K. Hall (ed.), Bone. Bone Growth-B, Vol. 7. CRC Press Incorporated, Boca Raton.

———, A. Grandin, A. Arbourachid, and A. de Ricqlès. 1996. Expression de la dynamique de croissance dans la structure de l'os périostique chez *Anas platyrhynchos.* Comptes-rendus de l'Académie des Sciences (Paris), Sciences de la Vie 319:301–308.

Chinsamy, A. 1990. Physiological implications of the bone histology of *Syntarsus rhodesiensis* (Saurischia:Theropoda). Palaeontologica Africana 27:77–82.

——— 1993. Bone histology and growth trajectory of the prosauropod dinosaur *Massospondylus carinatus* Owen. Modern Geology 18: 319–329.

——— 1995. Ontogenetic changes in the bone histology of the Late Jurassic ornithopod *Dryosaurus lettowvorbecki.* Journal of Vertebrate Paleontology 15:96–104.

Colbert, E. H. 1962. The weights of dinosaurs. American Museum Novitates 2076:1–16.

Coombs, W. P., Jr. 1975. Sauropod habits and habitats. Palaeogeography, Palaeoclimatology, Palaeoecology 17:1–33.

Crompton, A. W., E. Robinson, and M. D. Shapiro. 1996. Bone growth and remodeling in the avian hind limb. Journal of Vertebrate Paleontology 16:64A.

Currey, J. D. 1962. The histology of the bone of a prosauropod dinosaur. Palaeontology 5:238–246.

Curry, K. A. 1994. Juvenile sauropods of the Morrison Formation of Montana. Journal of Vertebrate Paleontology 14:22A.

——— 1996. Diplodocid osteogenesis. Journal of Vertebrate Paleontology 16:29A.

——— 1998. Histological quantification of growth rates in *Apatosaurus.* Journal of Vertebrate Paleontology 15:36–37A.

Dodson, P. 1990. Sauropod paleoecology; pp. 402–407 *in* D. B. Weishampel, P. Dodson, and H. Osmolska (eds.), The Dinosauria. University of California Press, Los Angeles.

Enlow, D. H. 1963. Principles of Bone Remodeling. Charles C. Thomas, Springfield, 123 pp.

——— and S. O. Brown. 1956. A comparative histological study of fossil and recent bone tissue (Part 1). Texas Journal of Science 8: 405–443.

——— and ——— 1957. A comparative histological study of fossil and recent bone tissue (Part 2). Texas Journal of Science 9:186–214.

——— and ——— 1958. A comparative histological study of fossil and recent bone tissue (Part 3). Texas Journal of Science 10:187–230.

Evans, F. G., and M. L. Riolo. 1970. Relations between the fatigue life and histology of adult human cortical bone. Journal of Bone and Joint Surgery 52A:1579.

Fawcett, D. W. 1942. Amedullary bones of the Florida Manatee (*Trichechus latirostris*). American Journal of Anatomy 71:271–303.

Ferguson, M. W. J., L. S. Honig, P. Bringas Jr., and H. C. Slavkin. 1982. In vivo and in vitro development of first branchial arch derivatives

in *Alligator mississippiensis*; pp. 275–286 *in* A. D. Dixon and B. Sarnat (eds.), Factors and Mechanisms Influencing Bone Growth. Alan R. Liss Incorporated, New York.

Foote, J. S. 1913. The comparative histology of the femur. Smithsonian Miscellaeous Collection 61(2232).

Francillon-Vieillot, H., V. de Buffrénil, J. Castanet, J. Géraudie, F. J. Meunier, J. Y. Sire, L. Zylberberg, and A. de Ricqlès. 1990. Microstructure and mineralization of vertebrate skeletal tissues; pp. 473–530 *in* J. G. Carter (ed.), Skeletal Biomineralization: Patterns, Processes, and Evolutionary Trends, Vol. 1. Van Nostrand Reinhold, New York.

Gilmore, C. W. 1936. Osteology of *Apatosaurus* with special reference to specimens in the Carnegie Museum. Memoirs of the Carnegie Museum XI(4):175–224.

Gross, W. 1934. Die Typen des mikroskopischen Knochenbaues bei fossilen Stegocephalen und Reptilien. Zeitschrift fur Anatomie 103: 731–764.

Hatcher, J. B. 1902. Structure of the forelimb and manus of *Brontosaurus*. Annals of Carnegie Museum I:356–376.

Horner, J. R., K. Padian, and A. de Ricqlès. 1997. Histological analysis of a dinosaur skeleton: evidence of skeletal growth variation. Journal of Morphology 232 (3):266.

Lacroix, P. 1971. The internal remodeling of bones; pp. 119–144 *in* G. H. Bourne (ed.), The Biochemistry and Physiology of Bone, Vol. 3. Academic Press, New York.

Martin, R. B., and D. B. Burr. 1989. Structure, Function, and Adaptation of Compact Bone. Raven Press, New York, 275 pp.

McIntosh, J. M. 1990a. Sauropoda; pp. 345–401 *in* D. B. Weishampel, P. Dodson, and H. Osmolska (eds.), The Dinosauria. University of California Press, Los Angeles.

——— 1990b. The second Jurassic dinosaur rush. Earth Sciences History 9:22–27.

McMahon, T. A., and J. T. Bonner. 1983. On Size and Life. Scientific American Library, New York, 255 pp.

Nopsca, F. 1933. On the histology of the ribs in immature and half-grown trachodont dinosaurs. Proceedings of the Zoological Society of London 1933:221–226.

Owen, R. 1859. Monograph on the fossil Reptilia of the Wealden and Purbeck Formations. Supplement II. Crocodilia (*Streptospondylus* etc.). Palaeontographic Society Monograph 11:20–44.

Peabody, F. E. 1961. Annual growth zones in vertebrates (living and fossil). Journal of Morphology 108:11–62.

Peterson, O. A., and C. W. Gilmore. 1902. *Elosaurus parvus*; a new genus and species of Sauropoda. Annals of Carnegie Museum I: 490–499.

Reid, R. E. H. 1981. Lamellar-zonal bone with zones and annuli in the pelvis of a sauropod dinosaur. Nature 292:49–51.

——— 1984. The histology of dinosaurian bone, and its possible bearing on dinosaurian physiology; pp. 629–663 *in* M. W. J. Ferguson (ed.), The Structure, Development and Evolution of Reptiles: Zoological Society of London Symposia 52. Academic Press, London.

——— 1990. Zonal "growth rings" in dinosaurs. Modern Geology 15: 19–48.

——— 1996. Bone Histology of the Cleveland-Lloyd dinosaurs and of dinosaurs in general (Part I): introduction to bone tissues. Brigham Young University Geology Studies 41:25–71.

——— 1997. How Dinosaurs Grew; pp. 403–413 *in* J. O. Farlow and M. K. Brett-Surman (eds.), The Complete Dinosaur. Indiana University Press, Bloomington and Indianapolis.

Rhodin, A. G. J. 1985. Comparative chondro-osseus development and growth of marine turtles. Copeia 1985:752–771.

Ricqlès, A. de. 1968a. Quelques observations paléohistologiques sur le dinosaurien sauropode *Bothriospondylus*. Annales of the University of Madagascar 6:157–209.

——— 1968b. Recherches paléohistologiques sur les os longs des tétrapodes. I—Origine du tissu osseux plexiforme des dinosauriens sauropodes. Annales de Paléontologie 54:133–145.

——— 1976. Recherches paléohistologiques sur les os longs des Tétrapodes. VII—Sur la classification, la signification fonctionnelle et l'histoire des tissus osseux des Tétrapodes (deuxieme partie: fonctions). Annales de Paléontologie (Vertébrés) 62:71–126.

——— 1977. Recherches paléohistologiques sur les os longs de-Tétrapodes. VII (deuxième partie: fonctions) (suite). Annales de Paléontologie (Vertébrés) 63:33–56, 133–160.

——— 1980. Tissue structure of dinosaur bone. Functional significance and possible relation to dinosaur physiology; pp. 103–139 *in* R. D. K. Thomas and E. C. Olson (eds.), A Cold Look at the Warm-Blooded Dinosaurs. AAAS Selected Symposium, Vol. 28. Westview Press, Boulder.

——— 1983. Cyclical growth in the long limb bones of a sauropod dinosaur. Acta Paleontologica 28:225–232.

——— and J. Bolt. 1983. Jaw growth and tooth replacement in *Captorhinus aguti* (Reptilia, Captohinomorpha): a morphological and histological analysis. Journal of Vertebrate Paleontology 3:7–24.

———, J. R. Horner, and K. Padian. 1997a. Histological evidences of dinosaur growth patterns (abstract); p. 172 *in* Z. Rocek and S. Hart (eds.), Herpetology 97—Abstracts of the Third World Congress of Herpetology. Prague.

———, K. Padian, and J. R. Horner. 1997b. Comparative biology and the bone histology of extinct tetrapods: what does it tell us? Journal of Morphology 232 (3):246.

———, F. J. Meunier, J. Castanet, and H. Francillon-Vieillot. 1991. Comparative micro-structure of bone; pp. 1–78 *in* B. K. Hall (ed.), Bone. Bone Matrix and Bone Specific Products, Vol. 3. CRC Press Incorporated, Boca Raton.

Rimblot-Baly, F., A. de Ricqlès, and L. Zylberberg. 1995. Analyse paléohistologique d'une série de croissance partielle chez *Lapparentosaurus madagascariensis* (Jurassique Moyen): Essai sur la dynamique de croissance d'un dinosaure sauropode. Annales de Paléontologie 81:49–86.

Sanchez-Herraiz, M. J., M. Esteban, J. Castanet, and R. Marquez. 1997. Age, size, and advertisement calls in two Spanish populations of *Pelodytes punctatus* (anura); p. 182 *in* Z. Rocek and S. Hart (eds.), Herpetology 97—Abstracts of the Third World Congress of Herpetology. Prague.

Seitz, A. L. 1907. Vergleichende Studien uber den mikroskopischen Knochenbau fossiler und rezenter Reptilien. Nova Acta Kaiser Leop.-Carol Deutschen Akademie fur Naturforschung 87:230–370.

Varricchio, D. J. 1993. Bone microstructure of the upper Cretaceous theropod dinosaur *Troodon formosus*. Journal of Vertebrate Paleontology 13:99–104.

Wells, J. W. 1963. Coral growth and geochronometry. Nature 197:948–950.

*Received 1 May 1998; accepted 1 May 1999.*

APPENDIX 1. Classification of Bone Tissue

Dinosaurian bone tissues exhibit a range of typologies equitable to that known in extant vertebrates. Several bone classificatory schemes have been established for extant bone structures, and have resulted in a sometimes confusing mix of terminology and systematic treatment of bone tissue identification (see Ricqlès et al., 1991 for an historical review). Descriptive terminology utilized in this analysis follows Ricqlès (1980). Only terms most relevant to dinosaurian bone histology are included.

I. Bone Formation (osteogenesis, ossification)
   A. Intramembranous Ossification. Bone tissue develops directly in vascularized mesenchyme. Cranial and flat facial bones and some pectoral girdle elements (clavicles) form intramembranously. Intramembranous ossification is typically associated with "dermal bones."
      1. Diploe refers to the adult morphology of intramembranous bones: a central cancellous zone is interposed between two layers of compact cortical bone. Diploe can also form in endochondral flat bones.
   B. Endochondral Ossification. Bone tissue is deposited in the central ossifying regions of cartilaginous forerunners of future bones. Long, short, and flat bones form endochondrally. Endochondral ossification is typically associated with the endoskeleton.
II. Bone Matrices (fibrillar organization of bone tissue)
   A. Periosteal bone matrices are deposited appositionally at the external margins of growing bones.
      1. Woven fibered matrices of periosteal origin contain collagen fibers of variable sizes that are loosely packed with poor spatial organization. Woven matrices are anisotropic under crossed Nichols in polarized light.
      2. Parallel fibered matrices of periosteal origin exhibit an intermediate organization of collagen fibers. Fibers are closely packed, arranged in the same general direction, and are highly anisotropic in polarized light.
      3. Lamellar fibered matrices of periosteal origin consist of highly organized superimposed lamellae. Within a single lamella, collagen fibers have a parallel orientation, but fiber directions vary among lamellae, to result in an alternating dark/light extinction pattern under crossed Nichols in polarized light.
   B. Osteonal bone matrices are also known as internal bone matrices and may form both within osteons and on the endosteal surfaces of bones.
      1. Primary osteons form by centripetal deposition of lamellar matrices within primary vascular canals.
      2. Secondary osteons (Haversian osteons, Haversian systems) form following local erosion and redeposition of pre-existing bone tissue. They may occur at the endosteal margins of bones during radial growth and medullary drift, or as intracortical secondary osteons (=Haversian systems sensu stricto). Peripheral reversal lines indicate the secondary nature of such structures.
III. Bone Tissues
   A. Primary compact bone tissues are formed by apposition in actively growing bones.
      1. Lamellar-zonal periosteal bone tissues usually exhibit parallel/lamellar fibered bone matrices. Vascularization may be lacking, but is generally scattered. When present, it consists of simple vascular canals and primary osteons. Evidence of cyclical growth is often extensively developed (see below).
      2. Woven periosteal bone tissues consist of a woven bone matrix with simple vascular canals. Vascularity may be dense. Woven bone is most common during embryological development, in regions of bone repair, and during rapid tissue production.
      3. The fibro-lamellar complex is identified by the presence of a woven bone matrix of periosteal origin containing lamellar primary osteons surrounding primary vascular canals.
   B. Secondary compact bone tissues are formed as a result of erosion and redeposition in pre-existing compact bone tissues. Reversal lines indicate the tissue's secondary nature.
      1. Haversian bone tissue forms from sequential erosion and redeposition of osteonal tissue and results in obliteration of underlying, older primary osteons.
      2. Non-Haversian perimedullar secondary tissues occur in perimedullar regions of bones during remodeling. These endosteal tissues are sometimes avascular and marked with multiple "growth lines."
IV. Bone Vascularization: classification of primary bone based on vascular canal orientation.
   A. Avascular (=nonvascular) primary bone most often occurs in the context of parallel/lamellar fibered matrices.
   B. Primary vascular canals in a single direction may be oriented longitudinally, circularly, radially, or obliquely to the long axis of a bone.
   C. Primary vascular canals in multiple directions intercalate in three basic patterns, regardless of the bone matrix in which they lie.
      1. Laminar vascularization (Foote, 1913) is characterized by primary canals oriented circularly and longitudinally in superimposed laminae, or vascular layers most often observed in the fibro-lamellar complex.
      2. Plexiform vascularization (Enlow, 1963) is laminar vascularization with the addition of radial vascular canals, to create a three-dimensional vascular plexus.
      3. Reticular vascularization is an obliquely and irregularly oriented vascular pattern often observed in the fibro-lamellar complex.
   D. Secondary vascular canals (secondary osteons). See above.
V. Growth Marks in dinosaurian tissues are divisible into three main categories, all representing a periodicity in bone deposition.
   A. Zones correspond to periods of active growth and osteogenesis. They do not necessarily represent annual cyclicity of bone deposition. Zones are thicker than annuli and lines of arrested growth (LAGs), and normally consist of woven to parallel-fibered matrices. In the fibro-lamellar complex, zones are composed of superimposed laminae.
   B. Annuli are narrower than zones and reflect periods of relatively slow growth rates. They are normally composed of parallel/lamellar fibered bone tissue, and may occur as thin rings in localized regions of cortical bone.
   C. Lines of Arrested Growth (LAGs) represent a period of temporary but complete cessation of appositional growth. LAGs are generally deposited at the surface of annuli, but can abruptly interrupt a sequence of laminae in the fibro-lamellar complex.